The effect of Wi-Fi on elastic and collagen fibres in the blood vessel wall of the chorioallantoic membrane

Katarína Holovská[1], Sandra Andrašková[1], Eva Petrovová[1], Ján Molnár[2], Tibor Vince[2], Viera Almášiová[1]

[1]University of Veterinary Medicine and Pharmacy, Department of Morphological Disciplines, Košice, Slovak Republic
[2]Technical University, Department of Theoretical and Industrial Electrical Engineering, Faculty of Electrical Engineering and Informatics, Košice, Slovak Republic

Received April 16, 2025
Accepted July 8, 2025

Abstract

In this study we observed the effect of Wi-Fi on various fibrous components that form the wall of large blood vessels in the chorioallantoic membrane (CAM) of the chicken embryo. Chicken embryos in the experimental groups (Wi-Fi) were continuously exposed (24 h per day) to Wi-Fi radiation at a frequency of 2.4 GHz and an average power density of 300 μW/m^2 for 9 and 14 embryonic days (ED). Subsequently, the CAM samples from the control (CO) and experimental (Wi-Fi) groups were histologically processed and evaluated. The samples stained with haematoxylin and eosin did not reveal any notable differences in the structure of large blood vessels between the CO and Wi-Fi groups. However, the use of special staining methods showed adverse effect of Wi-Fi on the fibrous elements within the blood vessel wall. The optical density (OD) of elastic fibres significantly decreased from 0.294 ± 0.025 (CO 9) to 0.197 ± 0.022 (Wi-Fi 9) at ED 9 and from 0.706 ± 0.028 (CO 14) to 0.271 ± 0.031 (Wi-Fi 14) at ED 14. On the other hand, at ED 9, the OD of collagen fibres exhibited a notable increase from 0.178 ± 0.023 (CO 9) to 0.334 ± 0.020 (Wi-Fi 9). However, at ED 14, there was a significant decline of collagen fibres from 0.418 ± 0.033 (CO 14) to 0.327 ± 0.031 (Wi-Fi 14). Our results support the hypothesis that Wi-Fi could affect the fibrous elements of the large vessel wall and may play a role in the development of different cardiovascular disorders.

Cardiovascular system, non-ionising electromagnetic radiation

Non-ionising electromagnetic radiation (EMR) has the potential to affect the human body at the biological level in a variety of ways (Dartnell 2011). Although EMR is part of nature (the sun, the earth and the ionosphere), technological advances over the last century have resulted in artificial sources becoming the main contributors to EMR in the environment (Karipidis et al. 2021). Artificial sources of EMR include various electronic devices such as printers, computers, hairdryers, refrigerators, televisions, mobile phones, satellite transmissions, and Wi-Fi, in addition to numerous other wireless communications (Ebrahim et al. 2016; Karipidis et al. 2021). These devices generate radiofrequency electromagnetic fields that can potentially pose a risk to human health (Abdulameer and Alsahlany 2022).

The chicken chorioallantoic membrane (CAM) is widely used in *in vivo* models for a range of research areas including angiogenesis, vascular disease, cancer therapies, wound healing, tissue transplantation, biomaterial engineering, drug development, genomics and more (Chen et al. 2021; Ribatti et al. 2021). Morphologically, the CAM is a highly vascularised membrane consisting of three layers: the chorionic epithelium, the mesenchyme and the allantoic epithelium. Each of these layers has a specific function (Makanya et al. 2016). The development of blood vessels in the CAM is a highly complex process. During this process, the vasculature of the CAM is subjected to continuous remodelling in order to meet the increasing metabolic demands of the chicken embryo. The mature CAM contains a rich vascular and lymphatic network, which is connected with the embryo by two allantoic arteries and one vein (Ribatti 2016; Kundeková et al. 2021). This can be considered

Address for correspondence:
doc. MVDr. Katarína Holovská, PhD.
Department of Morphological Disciplines
University of Veterinary Medicine and Pharmacy
Komenského 73, 041 81 Košice, Slovak Republic
Phone: +421 915 984 696
E-mail: katarina.holovska@uvlf.sk
http://actavet.vfu.cz/

an analogy to the umbilical arteries and veins observed in mammals (Merckx et al. 2020). In general, the mature vessel wall is organised into three basic layers which are known as the tunica interna-intima, the tunica media, and the tunica externa-adventitia. The primary component of the mature vessel wall is the extracellular matrix (ECM), which is composed of individual molecules secreted by the cells that constitute the vascular wall. The ECM is constituted of two principal molecular types: fibrous proteins and glycosaminoglycans (GAGs). The fibrous proteins are composed of elastin, collagen, and laminin (Rhodes and Simons 2007).

Elastin represents the primary component of elastic fibres, which provide the elasticity necessary for the proper functioning of large arteries. Elastin is synthesised by smooth muscle cells in the tunica media (Hungerford et al. 1996), although it can also be produced by endothelial cells in the tunica intima (Cantor et al. 1980; Cocciolone et al. 2018), as well as fibroblasts in the tunica adventitia (Ruckman et al. 1994). In the tunica media of large arteries, elastin is present in the form of elastic fibres or elastic lamellae (Wagenseil and Mecham 2009; Fhayli et al. 2019). The number of concentric elastic lamellae diminishes downstream of the vascular tree. It has been observed that the ascending aorta of the rat contains 10–13 concentric lamellar units, 1–3 in the iliac femoral arteries and 0 in smaller arteries (Awal et al. 1995). It is established that elastic fibres are highly stable over time, with a half-life of several decades (Sherratt 2009), and demonstrate particular resilience to chemical and physical assaults (Lillie et al. 1994). However, they can be degraded by elastin-degrading enzymes whose syntheses and activations are subject to modulation by a number of intrinsic and extrinsic factors (Sherratt 2009; Fhayli et al. 2019). Subsequently, a deficiency of elastin or disorganisation, improper assembly, and fragmentation of elastic fibres result in alterations to their function (Cocciolone et al. 2018).

Collagen is a highly rigid protein that constrains vessel distension (Kong et al. 2013; Xu and Shi 2014). The most prevalent collagens in the vascular wall are types I and III (Howard and Macarak 1989). Type I collagen provides resistance to stretching, whereas type III collagen forms a network that offers resilience and structural maintenance of the vessel wall (Shabani et al. 2024). Moreover, collagens play a pivotal role in vascular cell physiology and pathophysiology (Pozzi et al. 1998), as well as in the process of tissue remodelling, and foetal development (Goldberg et al. 2007; Parkin et al. 2017). Conversely, an excess of collagen in the vascular wall can result in the formation of fibrosis and an increased stiffness of the vessel (Xu and Shi 2014). It is known that reticular fibres are of the type III collagen family (Alvarenga and Marti 2014). It has been observed that they develop as the first in each tissue containing these fibres. As the fibres mature, they are largely replaced by stronger type I collagen fibres. Additionally, they facilitate the early synthesis of the extracellular matrix during wound healing, scar tissue formation, and embryonic development (Kuloğlu 2022).

According to the available literature, this work is a pioneering study of the influence of Wi-Fi on the fibrous components of the blood vessel wall in the CAM, and is therefore highly original and valuable. Currently, there is a lack of data on the impact of Wi-Fi on the fibrous components which play a key role in vascular function. It is known that an imbalance of fibres in the blood vessel wall can precipitate the onset of a range of cardiovascular diseases (Wagenseil and Mecham 2012; Heinz 2020). Therefore, the present study examined the extent to which these fibres might be influenced by EMR, the source of which is Wi-Fi. EMR is regarded as one of the most rapidly expanding anthropogenic factors affecting the human body in various ways (Karipidis et al. 2021), and therefore further research in this area is needed.

Materials and Methods

Ethical statement

In accordance with Directive 2010/63/EU, the use of the chicken embryo as an animal model does not necessitate ethical committee approval for animal experimentation (Directive 2010/63/EU).

Experimental design

Fertilized chicken eggs (*Gallus gallus domesticus*, Lohmann Brown breed, n = 60) were purchased from the chicken farm Párovské Háje, Nitra, Slovak Republic and delivered in a temperature-controlled manner to ensure their viability and quality. The eggs were randomly divided into two control groups CO 9 (n = 15) and CO 14 (n = 15) and two Wi-Fi groups that were continuously exposed (24 h per day) to the radiation with a frequency of 2.4 GHz and an average power density of 300 μW/m^2 during 9 (Wi-Fi 9, n = 15) and 14 (Wi-Fi 14, n = 15) embryonic days (Wi-Fi exposure system, Almášiová et al. 2024). The eggs were incubated horizontally in a forced-draft constant-humidity incubator at 37.5 ± 0.5 °C and 60% relative humidity (ET 49, River Systems, Campodarsego, Italy). On ED 9 and ED 14, samples of the chorioallantoic membranes of the controls and Wi-Fi groups were collected and processed for light microscopy.

Histopathological analysis – light microscopy

The samples for light microscopy were fixed using Dent's fixative (80% methanol, Mikrochem, Pezinok, Slovak Republic; 20% DMSO, Honeywell, Charlotte, USA), dehydrated through a successive alcohol series, and finally embedded in paraffin wax. Tissue sections (5–7 μm) were stained with haematoxylin and eosin for observation of the general histological structure. Additionally, various fibre types in the CAM were quantified using a commercially available kit, in accordance with the instructions provided by the manufacturer. Collagen identification was achieved by the use of Picrosirius red (0.1% Picrosirius red in saturated aqueous picric acid; Sigma-Aldrich, Saint Louis, USA), while the Weigert long method (Bio-Optica, Milano, Italy) was utilised for the identification of elastic fibres. The confirmation of reticular fibres was achieved using the Gordon-Sweet method (Bio-Optica). The sections were examined under a light microscope (Olympus CX43, Tokyo, Japan) and documented with a camera (Promicra, Prague, Czech Republic).

Morphometric analysis - collagen, elastic fibres, and reticular fibres quantification

The optical density (OD) of collagen, elastic fibres, and reticular fibres in the walls of the large blood vessels was calculated and compared between control groups and Wi-Fi groups. The images were generated and saved in TIFF format to facilitate enhanced resolution. Subsequently, the images were converted to greyscale 8-bit images using ImageJ 1.8.0_112 and analysed morphometrically as follows: the blood vessels in the CAM samples (6 samples per group) were analysed under × 40 magnification. Furthermore, the results were averaged and subjected to evaluation. The morphometric analysis of the randomised blood vessels (8–10 per sample) is based on the quantification of 8–10 different areas within the blood vessel wall. The mean values were calculated from all these measurements. A total of 120 measurements were taken for the evaluation of the OD of the blood vessel wall. The measurements were taken using the multiple imaging software ImageJ (version 7.0, USA).

The elastin/collagen (ELN/COL) ratio was calculated by dividing the optical OD of elastin by the corresponding data for collagen (Basu et al. 2010).

Statistical analysis

The statistical analysis was performed using one-way ANOVA with Sidak's multiple comparisons test using GraphPad Prism 10 software (Dotmatics, Boston, MA, USA). All measurements were reported as mean ± standard deviation (SD). The differences were considered significant at P value < 0.0001.

Results

Histopathological analysis – light microscopy

Control groups (CO 9, CO 14)

On ED 9, the CAM was comprised of three layers: the chorionic epithelium, the allantoic epithelium, and the connective tissue layer (mesenchyme). The CAM exhibited a diversity of blood vessels of varying calibre, distributed throughout the mesenchyme. The wall of the large blood vessels was thin and consisted of an endothelial cells and inconspicuous layer of mesenchyme (Plate VI, Fig. 1A). The identification of elastic, collagen, and reticular fibres was achieved through the application of three special staining methods.

All types of fibres constituted a fine, weakly staining network throughout the CAM. Elastic and collagen fibres were observed beneath the allantoic epithelium, while reticular fibres were predominantly present in close contact with the chorionic epithelium. Furthermore, all types of fibres were identified within the walls of the large blood vessels (their OD is shown in Table 1). The elastic vascular components were the most prominent and intensely stained, arranged into 1–2 thicker lamellae that were interconnected by thinner elastic fibres. In contrast, the collagen and reticular fibres were weakly stained, forming a supporting network for the vessel wall (Plate VII, Fig. 2A-C).

Table 1. Values of the optical density of elastic, collagen, and reticular fibres in the wall of large blood vessels of the CAM.

	Elastic fibres mean ± SD		Collagen fibres mean ± SD		Reticular fibres mean ± SD	
	ED 9	ED 14	ED 9	ED 14	ED 9	ED 14
CO	0.294 ± 0.025	0.706 ± 0.028	0.178 ± 0.023	0.418 ± 0.033	0.199 ± 0.028	0.468 ± 0.016
Wi-Fi	0.197 ± 0.022*	0.271 ± 0.031*	0.334 ± 0.020*	0.327 ± 0.031*	0.205 ± 0.028	0.263 ± 0.018*

Data were presented as means ± standard deviation (SD); *$P < 0.0001$.
ED - embryonic day, CO - control group, Wi-Fi - group exposed to non-ionizing electromagnetic radiation.
Significant differences are marked with an asterisk.

On ED 14, both covering epithelia of the CAM were well developed. The wall of the large blood vessels was observed to exhibit the typical appearance and to be composed of three layers (tunica interna, tunica media, tunica adventitia). The tunica interna was composed of endothelial cells with oval nuclei that protruded into the lumen and thin layer of subendothelial connective tissue. The tunica media was thick and well developed, consisting of several layers of smooth muscle cells surrounded by extracellular matrix. The tunica adventitia was thin and exhibited a smooth transition into the surrounding mesenchyme (Plate VI, Fig. 1B).

In the entire connective tissue layer of the CAM and in the wall of large blood vessels, all types of fibres were stained more intensely compared to ED 9 (Plate VII, Fig. 3A-C). The tunica media was observed to contain three to four darkly stained, thick, circularly arranged elastic lamellae, which exhibited no consistent thickness and were irregularly arranged. The thin elastic fibres that were present among the elastic lamellae also extended into the surrounding connective tissue of the CAM. The collagen fibres were arranged in a circular pattern, forming thick, dark-staining lines. In addition, thinner collagen fibres extended into the surrounding connective tissue of the CAM. The reticular fibres constituted a fine supporting meshwork of the vessel wall that was very well developed. Furthermore, a significant increase in the OD of all types of fibres in the blood vessel wall was noted in comparison to ED 9 (Table 1). Specifically, the OD of collagen fibres increased by 34%, elastic fibres increased by 40%, and reticular fibres increased by 35%.

Experimental groups (Wi-Fi 9, Wi-Fi 14)

No significant differences were observed in the histological structure of the covering epithelium and connective tissue components of the CAM between the groups exposed to wireless connections (Wi-Fi 9, Wi-Fi 14) and the respective control groups (CO 9, CO 14). Furthermore, the morphology of the major blood vessels remained unchanged in all examined groups (Plate VI, Fig. 1C-D). However, the special staining methods revealed significant differences in the fibrous components of the vessel wall in the CAM between the CO and Wi-Fi groups.

In the Wi-Fi 9 group, the elastic fibres in the vessel wall were not arranged into the thick lamellae that were observed in the CO 9 group. The elastic fibres formed a delicate network that extended into the surrounding connective tissue. The collagen component was intensely stained in the vessel walls as well as in connective tissue close to the chorionic epithelium. Thick collagen fibres were clearly visible in both mentioned areas. The arrangement and staining intensity of reticular fibres were identical to those observed in the CO 9 group (Plate VII, Fig. 2D-F). The OD of elastic fibres in the blood vessel walls exhibited a notable decline (0.197 ± 0.022 in Wi-Fi 9 vs. 0.294 ± 0.025 in CO 9), whereas the OD of collagen fibres demonstrated a marked increase (0.334 ± 0.020 in Wi-Fi 9 vs. 0.178 ± 0.023 in CO 9). No significant difference was observed in the OD of reticular fibres between groups (0.205 ± 0.028 in Wi-Fi 9 vs. 0.199 ± 0.028 in CO 9) (Table 1).

In the Wi-Fi 14 group, all three types of fibres exhibited a reduction in staining intensity as well as OD in comparison to the control groups (CO 14) (Plate VII, Fig. 3D-F, Table 1). Marked changes were seen in the elastic lamellae, which exhibited a notable reduction in thickness and were only slightly stained. The OD of elastic fibres (0.271 ± 0.031 in Wi-Fi 14, vs. 0.706 ± 0.028 in CO 14), collagen fibres (0.327 ± 0.031 in Wi-Fi 14, vs. 0.418 ± 0.033 in CO 14), and reticular fibres (0.263 ± 0.018 in Wi--Fi 14, vs. 0.468 ± 0.016 in CO 14) in the large blood vessel wall significantly decreased in Wi-Fi group in comparison to the CO 14 group.

In the control groups, the elastin/collagen ratio (ELN/COL) of the large vessel walls was 1.651 in CO 9 and 1.684 in CO 14. A significant reduction in the ELN/COL ratio was observed in both exposed groups, namely, 0.589 for the Wi-Fi 9 group and 0.828 for the Wi-Fi 14 group.

Discussion

The mechanical properties of blood vessels are determined by the structural components that form their walls (Fhayli et al. 2019). The principal structural characteristics associated with the functionality of blood vessels are tensile stiffness, elasticity and compressibility. The extracellular matrix that constitutes the blood vessel wall is primarily composed of elastin, collagen (types I and III), some proteoglycans, and glycoproteins. Elastin is responsible for the flexibility of the vessel wall, while collagen provides tensile strength and resistance against rupture (Buttafoco et al. 2006).

Our results are in accordance with the above statements and also indicate that the elastic fibres represent the most prominent fibrous component of the blood vessels. In the control groups, the OD of elastic fibres in the vessels increased as the CAM matured, from 0.294 ± 0.025 on ED 9 to 0.706 ± 0.028 on ED 14. The elastic components were arranged into one or two thicker lamellae, which were interconnected by thinner elastic fibres. The collagen fibres and reticular fibres were less prominent but they constituted a supporting network for the vessel wall. On ED 14, the blood vessel wall was much thicker and fully developed. The quantity of all types of fibres exhibited a significant increase. In the tunica media, thick elastic lamellae (3–4) and collagen and reticular fibres were clearly visible. Under normal conditions, mature elastic fibres are capable of enduring throughout the entirety of an organism's lifespan. They are regarded as the most resilient component of the ECM (Arribas et al. 2006; Xu and Shi 2014). However, our observations indicated that exposure to Wi-Fi had a detrimental impact on elastic fibres and the other fibrous components that constitute the blood vessel wall. The OD of elastic fibres in the vessel wall was significantly decreased at ED 9 (Wi-Fi 9: 0.197 ± 0.022) and ED 14 (Wi-Fi 14: 0.271 ± 0.031). The damage to elastic fibres in blood vessels, together with additional biological processes, may be a contributory factor in the development of severe pathological conditions, including cardiovascular diseases such as atherosclerosis (Maurice et al. 2013; Heinz 2020). The degradation products of fragmented elastic fibres have been demonstrated to possess significant chemical signalling properties (Cocciolone et al. 2018). As elastic fibres are gradually damaged, their load-bearing function is presumably taken over by collagen, which results in a reduction in vessel wall elasticity and an increase in rigidity (Hodis and Zamir 2009). It has been documented that the production and reorganization of collagens in blood vessels is frequently observed in response to defects in or degradation of elastic fibres (Wan et al. 2010). Similar alterations in collagen fibres were observed in our study in response to Wi-Fi exposure. The extent of these changes depended on the ED. On ED 9, the OD of the collagen fibres exhibited a significant increase from 0.178 ± 0.023 (CO 9) to 0.334 ± 0.020 (Wi-Fi 9). However, this subsequent increase was followed by a significant decrease from 0.418 ± 0.033 (CO 14) to 0.327 ± 0.031

on ED 14 (Wi-Fi 14). Furthermore, additional collagen deposition or a shift in the ratio of different types of collagen in the wall may result in increased wall stiffness, which could subsequently affect the function of the vessel wall (Wagenseil and Mecham 2012).

As previously stated, collagen and elastin are two essential components of blood vessels, playing a pivotal role in their functionality (Basu et al. 2010). It has been observed that not only the quantity of fibres but also the ELN/COL ratio represents an interesting indicator of the quality of the blood vessel wall. However, the existing literature offers only limited insight into the investigation of ELN/COL ratios in different blood vessels. Basu et al. (2010) observed the ELN/COL ratio in different blood vessels of rats. The ELN/COL ratio in the aorta was 1.18 ± 0.02; in the carotid artery, the ratio was 1.03 ± 0.4; in the femoral artery and vena cava, the ratio was 0.61 ± 0.1 and 0.57 ± 0.1, respectively. Blood vessels with high blood flow always showed a higher ELN/COL ratio in comparison with blood vessels with low blood flow. Additionally, it was observed that the quantity of fibres and the ELN/COL ratio undergo changes throughout the lifespan. Some authors have observed an increase in the ELN/COL ratio in the human aorta, from 0.51 at age 14 to 0.6 at age 40 and 0.71 at age 90 (Andreotti et al. 1985; Wittig and Szulcek 2021). In contrast, a reduction in the ELN/COL ratio in ascending aortas was observed in another study, with a ratio of 1.65 in individuals aged 0–20 and 1.15 in those aged 70–100 (Hosoda et al. 1984). Moreover, animal models have demonstrated a reduction in the ELN/COL ratio in the context of pathological conditions such as hypertension (Arribas et al. 2006; Wittig and Szulcek 2021). We also observed significant alterations in the ELN/COL ratio in large vessel walls as a consequence of Wi-Fi exposure. In both experimental groups, there was a notable decline in the ELN/COL ratio, from 0.1651 to 0.589 in Wi-Fi 9 and from 1.684 to 0.828 in Wi-Fi 14. It has been observed that alterations in the fibrous components of the vessel wall may result in increased arterial stiffness and reduced arterial distensibility (Greenwald 2007). Such alterations can subsequently cause serious chronic inflammation and an increase in morbidity and mortality through the development and progression of various cardiovascular diseases (Heinz 2020).

The originality of our results is evidenced by the rarity, or complete absence, of studies with a similar focus. The objective of this study was to identify the various types of fibres in the wall of large blood vessels in CAM by using special staining methods. Subsequently, the fibres were quantified using the optical density method. Following a comparison of the control and experimental groups revealed significant changes in fibre quantity and their ratio (ELN/COL) due to Wi-Fi exposure.

In conclusion, this study is one of the first to suggest that Wi-Fi could possibly have an impact on the structural and mechanical properties of blood vessels. Given the constant exposure to non-ionising electromagnetic radiation, there is a potential risk of damage to various tissues in the body. The present study was designed to examine the effect of 2.4 GHz Wi-Fi radiation with an average power density of 300 $\mu W/m^2$ on the structure of the large blood vessel wall in the CAM. It was observed that continuous exposure to Wi-Fi had a detrimental effect on the fibrous components of the ECM. The amount and ELN/COL ratio of elastic, collagen and reticular fibres were found to be significantly altered, which may result in increased stiffness of the vessel wall. Based on our findings and the existing literature, we can assume that Wi-Fi may ultimately contribute to the pathogenesis of various cardiovascular diseases.

When interpreting our results, the limitations arising of the model used should also be taken into account. Although the CAM is an excellent model, it does not permit long-term monitoring. Other significant limitations include substantial differences in the physiology of embryos and adults, and the evolutionary divergence between chickens and humans.

Acknowledgements

This work was supported by the Slovak Research and Development Agency under the Contract no. VEGA 1/0036/22.

References

Abdulameer J, Alsahlany AM 2022: Review: Electromagnetic radiation effects on the human tissues. NeuroQuantology **20**: 8130-8146

Almášiová V, Andrašková S, Bučko M, Holovská K 2024: Effect of electromagnetic Wi-Fi radiation on the development of chicken embryo. Folia Vet **68**: 60-66

Alvarenga HG, Marti L 2014: Multifunctional roles of reticular fibroblastic cells: More than meets the eye? J Immunol Res **10**: 11-15

Andreotti L, Bussotti A, Cammelli D, di Giovine F, Sampognaro S, Sterrantino G, Varcasia G, Arcangeli P 1985: Aortic connective tissue in ageing—A biochemical study. Angiology **63**: 872-879

Arribas SM, Hinek A, Gonzalez MC 2006: Elastic fibres and vascular structure in hypertension. Pharmacol Ther **111**: 771-791

Awal MA, Matsumoto M, Nishinakagawa H 1995: Morphometrical changes of the arterial walls of main arteries from heart to the abdomino-inguinal mammary glands of rat from virgin through pregnancy, lactation and post-weaning. J Vet Med Sci **57**: 251-256

Basu P, Sen U, Tyagi N, Tyagi SC 2010: Blood flow interplays with elastin: collagen and MMP: TIMP ratios to maintain healthy vascular structure and function. Vasc Health Risk Manag **6**: 215-228

Buttafoco L, Kolkman NG, Buijtenhuijs PE, Poot AA, Dijkstra PJ, Vermes I, Feijen J 2006: Electrospinning of collagen and elastin for tissue engineering applications. Biomaterials **27**: 724-734

Cantor JO, Keller S, Parshley MS, Darnule TV, Darnule AT, Cerreta JM, Turino GM, Mandl I 1980: Synthesis of crosslinked elastin by an endothelial cell culture. Biochem Biophys Res Commun **95**: 1381-1386

Chen L, Wang S, Feng Y, Zhang J, Du Y, Zhang J, Ongeval CV, Ni Y, Li Y 2021: Utilisation of chick embryo chorioallantoic membrane as a model platform for imaging-navigated biomedical research. Cells **10**: 1-40

Cocciolone AJ, Hawes JZ, Staiculescu MC, Johnson EO, Murshed M, Wagenseil JE 2018: Elastin, arterial mechanics, and cardiovascular disease. Am J Physiol Heart Circ Physiol **315**: 189-205

Dartnell LR 2011: Ionizing radiation and life. Astrobiology **11**: 551-582

Ebrahim S, Azab AE, Albasha MO, Albishti N 2016: The biological effects of electromagnetic fields on human and experimental animals. IRJNAS **3**: 106-121

Fhayli W, Boëté Q, Harki O, Briançon-Marjollet A, Jacob MP, Faury G 2019: Rise and fall of elastic fibers from development to aging. Consequences on arterial structure-function and therapeutical perspectives. Matrix Biol **84**: 41-56

Goldberg SR, Quirk GL, Sykes VW, Kordula T, Lanning DA 2007: Altered procollagen gene expression in mid-gestational mouse excisional wounds. J Surg Res **143**: 27-34

Greenwald SE 2007: Ageing of the conduit arteries. J Pathol **211**: 157-172

Heinz A 2020: Elastases and elastokines: elastin degradation and its significance in health and disease. Crit Rev Biochem Mol Biol **55**: 252-273

Hodis S, Zamir M 2009: Mechanical events within the arterial wall: the dynamic context for elastin fatigue. J Biomech **42**: 1010-1016

Hosoda Y, Kawano K, Yamasawa F, Ishii T, Shibata T, Inayama S 1984: Age-dependent changes of collagen and elastin content in human aorta and pulmonary artery. Angiology **35**: 615-621

Howard PS, Macarak EJ 1989: Localization of collagen types in regional segments of the fetal bovine aorta. Lab Invest **61**: 548-555

Hungerford JE, Owens GK, Argraves WS, Little CD 1996: Development of the aortic vessel wall as defined by vascular smooth muscle and extracellular matrix markers. Dev Biol **178**: 375-392

Karipidis K, Brzozek C, Bhatt CR, Loughran S, Wood A 2021: What evidence exists on the impact of anthropogenic radiofrequency electromagnetic fields on animals and plants in the environment? A systematic map protocol. Environ Evid **10**: 1-9

Kong CH, Lin XY, Woo CC, Wong HC, Lee CN, Richards AM, Sorokin VA 2013: Characteristics of aortic wall extracellular matrix in patients with acute myocardial infarction: tissue microarray detection of collagen I, collagen III and elastin levels. Interact Cardiovasc Thorac Surg **16**:11-15

Kuloğlu HY 2022: Determination of reticular fibers in tissues fixed with sugarcane molasses. Journal of Advances in VetBio Science and Techniques. J Adv VetBio Sci Tech **7**: 361-365

Kundeková B, Máčajová M, Meta M, Čavarga I, Bilčík B 2021: Chorioallantoic membrane models of various avian species: differences and applications. Biology (Basel) **10**: 1-24

Lillie MA, Chalmers GW, Gosline JM 1994: The effects of heating on the mechanical properties of arterial elastin. Connect Tissue Res **31**: 23-35

Makanya AN, Dimova I, Koller T, Styp-Rekowska B, Djonov V 2016: Dynamics of the developing chick chorioallantoic membrane assessed by stereology, allometry, immunohistochemistry and molecular analysis. PLoS One **11**: 1-23

Maurice P, Blaise S, Gayral S, Debelle L, Laffargue M, Hornebeck W, Duca L 2013: Elastin fragmentation and atherosclerosis progression: the elastokine concept. Trends Cardiovasc Med **23**: 211-221

Merckx G, Tay H, Lo Monaco M, van Zandvoort M, De Spiegelaere W, Lambrichts I, Bronckaers A 2020: Chorioallantoic membrane assay as model for angiogenesis in tissue engineering: focus on stem cells. Tissue Eng Part B Rev **26**: 519-539

Parkin JD, San Antonio JD, Persikov AV, Dagher H, Dalgleish R, Jensen ST, Jeunemaitre X, Savige J 2017: The collagen III fibril has a "flexi-rod" structure of flexible sequences interspersed with rigid bioactive domains including two with hemostatic roles. PLoS One **12**: 1-24

Pozzi A, Wary KK, Giancotti FG, Gardner HA 1998: Integrin alpha1beta1 mediates a unique collagen-dependent proliferation pathway *in vivo*. J Cell Biol **142**: 587-594

Ribatti D 2016: The chick embryo chorioallantoic membrane (CAM). A multifaceted experimental model. Mech Dev **141**: 70-77

Ribatti D, Tamma R, Annese T 2021: Chorioallantoic membrane vascularization. A meta-analysis. Exp Cell Res **405**: 1-7

Rhodes JM, Simons M 2007: The extracellular matrix and blood vessel formation: not just a scaffold. J Cell Mol Med **11**: 176-205

Ruckman JL, Luvalle PA, Hill KE, Giro MG, Davidson JM 1994: Phenotypic stability and variation in cells of the porcine aorta: collagen and elastin production. Matrix Biol **14**: 135-145

Shabani Z, Schuerger J, Zhu X, Tang C, Ma L, Yadav A, Liang R, Press K, Weinsheimer S, Schmidt A, Wang C, Sekhar A, Nelson J, Kim H, Su H 2024: Increased collagen I/collagen III ratio is associated with hemorrhage in brain arteriovenous malformations in human and mouse. Cells **13**: 1-17

Sherratt MJ 2009: Tissue elasticity and the ageing elastic fibre. Age **31**: 305-325

Wagenseil JE, Mecham RP 2009: Vascular extracellular matrix and arterial mechanics. Physiol Rev **89**: 957-989

Wagenseil JE, Mecham RP 2012: Elastin in large artery stiffness and hypertension. J Cardiovasc Transl Res **5**: 264-273

Wan W, Yanagisawa H, Gleason RL Jr. 2010: Biomechanical and microstructural properties of common carotid arteries from fibulin-5 null mice. Ann Biomed Eng **38**: 3605-3617

Wittig C, Szulcek R 2021: Extracellular matrix protein ratios in the human heart and vessels: How to distinguish pathological from physiological changes? Front Physiol **12**: 1-9

Xu J, Shi GP 2014: Vascular wall extracellular matrix proteins and vascular diseases. Biochim Biophys Acta **1842**: 2106-2119

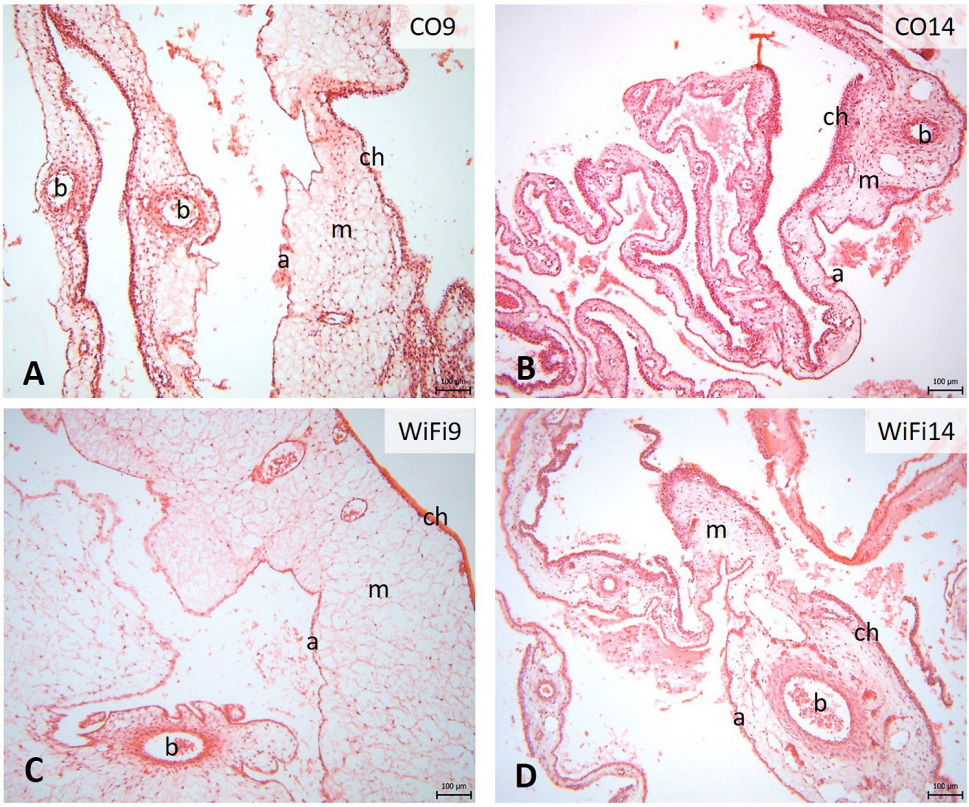

Fig. 1. Microphotographs representative of the chorioallantoic membrane on embryonic day 9 (A, C) and on embryonic day 14 (B, D). CO9 - control group on embryonic day 9; CO14 - control group on embryonic day 14; WiFi9 - group exposed to Wi-Fi on embryonic day 9; WiFi14 - group exposed to Wi-Fi on embryonic day 14; a - allantoic epithelium; b - blood vessel; ch - chorionic epithelium; m - mesenchyme. Sections were stained with haematoxylin and eosin. Scale bar = 100 μm.

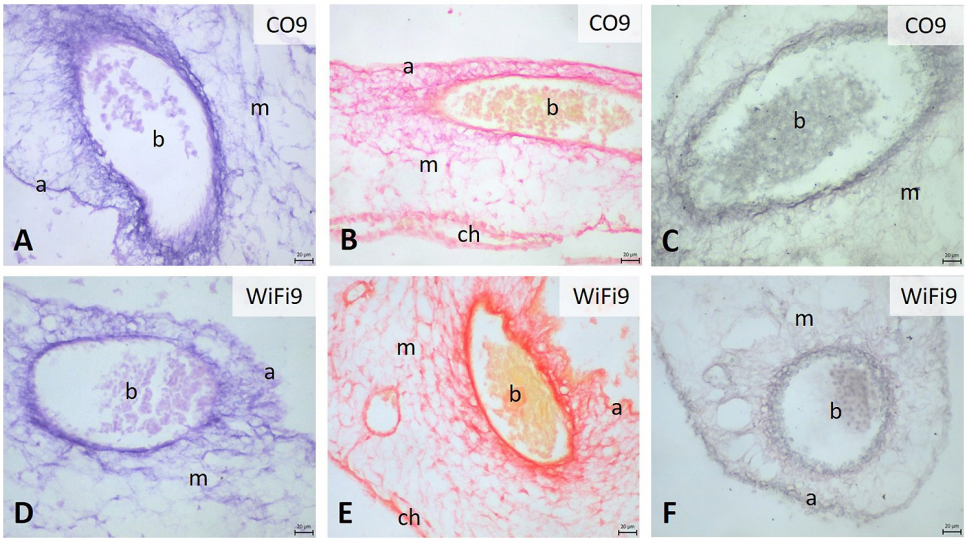

Fig. 2. Microphotographs representative of the chorioallantoic membrane on the embryonic day 9 from control (CO9: A, B, C) and Wi-Fi (WiFi9: D, E, F) groups. CO9 - control group on embryonic day 9; WiFi9 - group exposed to Wi-Fi on embryonic day 9; a - allantoic epithelium; b - blood vessel; ch - chorionic epithelium; m - mesenchyme. Sections were stained with Weigert (A, D), Picrosirius red (B, E), and Gordon-Sweet (C, F) methods. Scale bar = 20 μm.

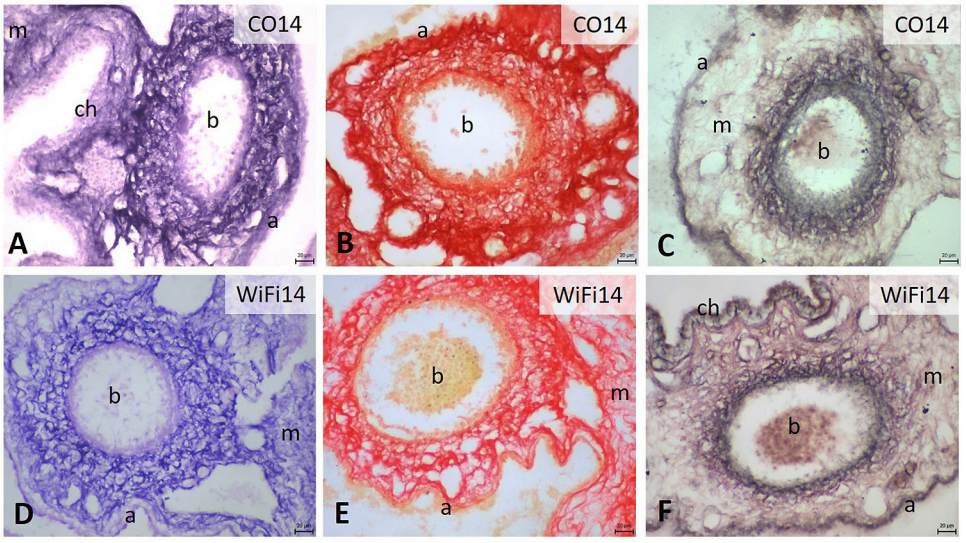

Fig. 3. Microphotographs representative of the chorioallantoic membrane on the embryonic day 14 from control (CO14: A, B, C) and Wi-Fi (WiFi14: D, E, F) groups. CO14 - control group on embryonic day 14; WiFi14 - group exposed to Wi-Fi on embryonic day 14. High magnification of the main blood vessels: a - allantoic epithelium; b - blood vessel; ch - chorionic epithelium; m - mesenchyme. Sections were stained with Weigert (A, D), Picrosirius red (B, E), and Gordon-Sweet (C, F) methods. Scale bar = 20 μm.